Studii şi Cercetări Ştiinţifice
Chimie şi Inginerie Chimică, Biotehnologii, Industrie Alimentară

Scientific Study & Research
Chemistry & Chemical Engineering, Biotechnology, Food Industry

2025, **26** (4), pp. 495 – 507

https://doi.org/10.29081/ChIBA.2025.663

ISSN 1582-540X

ORIGINAL RESEARCH PAPER

HYDROCHEMICAL ANALYSIS OF A SHALLOW ALLUVIAL AQUIFER BETWEEN THE SIRET AND MOLDOVA RIVERS

Petrut-Liviu Bogdan[1*], Valentin Nedeff[1, 2*], Mirela Panainte-Lehadus[1], Narcis Barsan[1], Florin Marian Nedeff[1], Diana-Carmen Mirila[1]

[1] "Vasile Alecsandri" University of Bacau, Faculty of Engineering, Calea Marasesti 157, Bacau, 600115, Romania
[2] "Gheorghe Ionescu Sisesti", Academy of Agricultural and Forestry Sciences Bucharest, 61 Marasti Blvd., 011464, Bucharest, Romania

*Corresponding authors: bogdan.p.liviu@gmail.com, vnedeff@ub.ro

Received: November, 21, 2025
Accepted: December, 12, 2025

Abstract: The paper examines groundwater from the area between the Siret and Moldova rivers. Data from 2021 and 2022 were used, taken from twelve monitoring wells. The main ions (Ca^{2+}, Mg^{2+}, Na^{+}, K^{+}, HCO_3^-, Cl^-, SO_4^{2-}, NO_3^-) were checked with basic statistics, boxplots and the Piper and Schoeller-Berkaloff diagrams. The ion values from the two years stay close. The higher ones appear only in a few wells, and those places have local factors that influence the water. The meq·L^{-1} values also fall in the same range in both years. Ca^{2+} and HCO_3^-, remain dominant in all samples. The two diagrams place the water in the Ca–HCO_3 field, with no major change from one year to the next. There is no sign of a larger chemical shift in the aquifer, and the small differences stay local. The data show a stable aquifer, and these values can help when the area is checked again in the future.

Keywords: *alluvial aquifer, hydrochemical facies, major ions, meq·L^{-1}, Piper diagram, Schoeller-Berkaloff*

INTRODUCTION

Groundwater in alluvial systems is influenced by different natural and human factors, and its chemical composition usually reflects the local lithology and the way water moves through the sediments [1, 2]. In many areas, groundwater is the main source of supply for both population and industry, and even more for the agricultural sector [3]. Because of this, any change in ion composition can have an effect on how the whole system evolves in time [1, 4]. These changes appear during the recharge of the aquifer, when water passes through the rocks in situ, when infiltration comes from the rivers, or when local anthropogenic influences are present [5]. Many times, these processes overlap, and the natural chemistry of the water can be modified in ways that are not easy to observe directly [4].

Several studies show that aquifers formed in sandy and gravel deposits with carbonate material usually develop a Ca–HCO_3 facies, with some local deviations depending on the geological layers or land use in the surroundings [6 – 11]. These variations can appear from one year to another, but in general the main facies keeps a stable form. Hydrochemical diagrams like Piper and Schoeller–Berkaloff are often used because they help to see how ions group together, even when the sampling network is not very dense [12 – 14]. Such diagrams can indicate points with different behavior or possible ion-exchange processes [15, 16].

The sector between the Siret and Moldova rivers has a shallow alluvial aquifer where groundwater circulates mainly through mixed sand and gravel layers. In the scientific literature, there are some works made on nearby or similar areas [17 – 22], but for this specific sector the behavior of the major ions and the stability of the facies were not described in much detail. The previous studies are useful for methodology, but they are not dedicated strictly to this area.

Because the monitoring network provides two consecutive datasets (2021 and 2022), the information allows a simple comparison of the ion values and the way they tend to group, without using interpolation methods that normally require more sampling points.

In this study, the focus is mainly on the hydrochemical behavior of the aquifer. The main ions (Ca^{2+}, Mg^{2+}, Na^{+}, K^{+}, HCO_3^-, Cl^-, SO_4^{2-} and NO_3^-) are analyzed at the sampling points, and the diagrams show how these ions appear together and if the facies keeps a similar structure in both years.

A simple point-based spatial representation is also included, together with a basic histogram that shows how the concentrations are spread in the two datasets. With this approach, the study offers a more process-oriented view of the aquifer and shows where small changes appear, how the facies behaves in a short time, and what hydrochemical tendencies may influence the system. The determination of the hydrogeochemical facies is carried out by interpreting the Piper and Schoeller-Berkaloff diagrams, which make it possible to observe how cations and anions associate at the sampled points and whether the chemical structure of the water remains consistent between the two years.

MATERIALS AND METHODS

Study area

The study area is located between the Siret and Moldova rivers, in the eastern part of Romania. The aquifer in this sector is shallow and develops mainly in mixed deposits of sand, gravel and thin clay layers [23]. Groundwater is recharged both from local rainfall and from the rivers, especially during periods with higher flow [24]. Most of the land is used for agriculture, and there are several small rural communities close to the area [25]. Even if the aquifer is not very deep, its behavior depends a lot on the local lithology and on the way the two rivers influence the groundwater level [26].

Data collection and sampling network

The groundwater quality, in the study area presented in Figure 1, was evaluated using the dataset provided by the National Administration “Apele Române- ABA Siret” [27]. The dataset includes measurements from 5 wells of the National Groundwater Monitoring Network (BH1 - BH5), together with 2 wells used for drinking-water supply (WD1, WD2), and 5 surveillance wells located in the industrial zone (WI1 - WI5) [17].
For the period 2021-2022, the main physico-chemical parameters were reported in these wells, and the values of the major ions were available for each sampling point: Ca^{2+}, Mg^{2+}, Na^{+}, K^{+}, HCO_3^-, Cl^-, SO_4^{2-} and NO_3^-.
These ions were selected because they are the base for most hydrochemical interpretations and are commonly used in facies studies. The annual average values were also calculated for each well, following the general requirements of Directive 2006/118/EC for groundwater quality [28] and Romanian Ordinance no. 7/2023 [29].

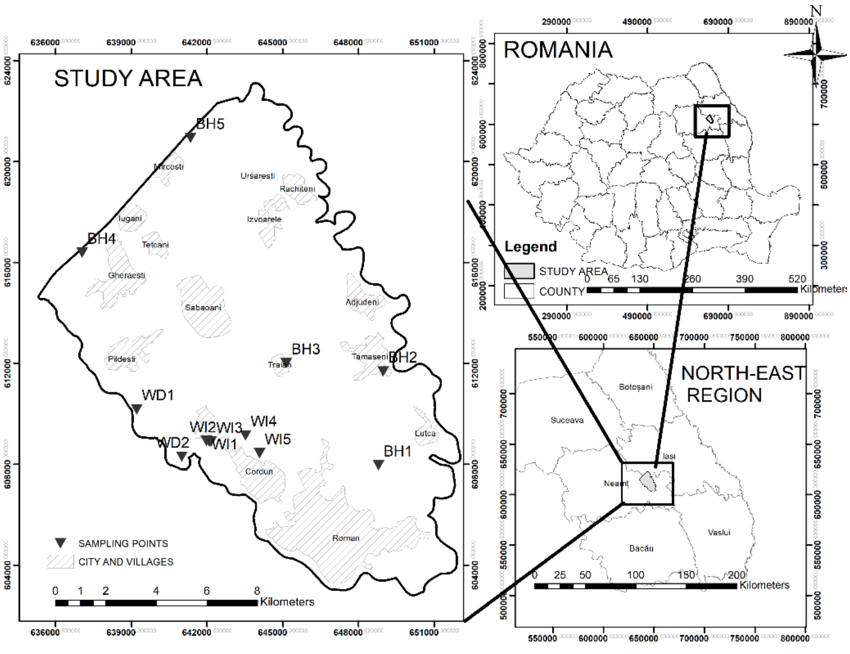

Figure 1. *Study area and sampling network*

The major ion concentrations were arranged into two separate tables, one for cations (Table 1) and one for anions (Table 2), together with the coordinates of the sampling points, in order to provide a clearer overview of the measured values for 2021 and 2022.

Table 1. *Major cations measured in the groundwater samples (2021-2022)*

No.	Sample point	Coordinates (stereo70)		CATIONS				Year
		X	Y	Ca^{2+} [$mg·L^{-1}$]	Mg^{2+} [$mg·L^{-1}$]	Na^{+} [$mg·L^{-1}$]	K^{+} [$mg·L^{-1}$]	
1	BH1	648789.46	607947.26	102.9	39.15	34.4	1.23	2021
2	BH2	648965.9	611672.02	232	26.25	68.1	14.2	2021
3	BH3	645126.58	611998.2	154	70.45	20.85	1.8	2021
4	BH4	637043.28	616381.77	143	30.85	19.5	4.1	2021
5	BH5	641338.54	620925.06	126.89	37.2	25.44	2.26	2021
6	WI1	639201.68	610166.45	131.99	36.7	25	1.6	2021
7	WI2	640991.53	608288.97	127.28	39.5	32	1.4	2021
8	WI3	641969.19	608919.29	99.23	41	36	1.3	2021
9	WI4	642081.89	608892.92	84	44	34	1.55	2021
10	WI5	642150.47	608880.95	102.4	43	35	1.45	2021
11	WD1	643513.36	609132.71	108	41.5	24	0.1	2021
12	WD2	644074.9	608429.77	85	37.5	26	0.1	2021
13	BH1	648789.46	607947.26	93.85	52.45	62.2	1.175	2022
14	BH2	648965.9	611672.02	178	43.25	93.5	15.5	2022
15	BH3	645126.58	611998.2	144	67.55	42.3	0.75	2022
16	BH4	637043.28	616381.77	145.5	28.45	47	3.3	2022
17	BH5	641338.54	620925.06	141.68	36	26.57	1.915	2022
18	WI1	639201.68	610166.45	103	46	59.2	1.4	2022
19	WI2	640991.53	608288.97	111	45	90.5	1.3	2022
20	WI3	641969.19	608919.29	113	49	39.3	1.1	2022
21	WI4	642081.89	608892.92	82.1	42	44	1.25	2022
22	WI5	642150.47	608880.95	101.3	38	23.57	1.2	2022
23	WD1	643513.36	609132.71	98	42	19.5	0.1	2022
24	WD2	644074.9	608429.77	106	38	26	0.2	2022

The values for the cations (Ca^{2+}, Mg^{2+}, Na^{+}, K^{+}) and anions (HCO_3^-, SO_4^{2-}, Cl^-, NO_3^-) used in the article represent the average annual measurements for each ion, and they were used like this to allow a clearer evaluation and comparison between the two years.
Boxplots were prepared for all major ions, grouped as cations and anions. By placing the values from 2021 and 2022 side by side, the differences between the two years become easier to observe, especially in terms of median position, data spread, and the presence of isolated higher values that may indicate local particularities.

Table 2. *Major anions measured in the groundwater samples (2021-2022)*

No.	Sample point	Coordinates (stereo70)		ANIONS				Year
		X	Y	HCO_3^- [mg·L^{-1}]	Cl^- [mg·L^{-1}]	SO_4^{2-} [mg·L^{-1}]	NO_3^- [mg·L^{-1}]	
1	BH1	648789.46	607947.26	488	58.8	54.6	23.79	2021
2	BH2	648965.9	611672.02	515.5	70.1	161.5	2.02	2021
3	BH3	645126.58	611998.2	622	70.1	37.5	135	2021
4	BH4	637043.28	616381.77	506	22.65	12.78	5.69	2021
5	BH5	641338.54	620925.06	461.5	58.085	52.92	2.7	2021
6	WI1	639201.68	610166.45	457	83.393	64.17	63.23	2021
7	WI2	640991.53	608288.97	569	77.053	103.67	31.33	2021
8	WI3	641969.19	608919.29	544	92.44	93.5	16.47	2021
9	WI4	642081.89	608892.92	549	83.195	64.5	31.55	2021
10	WI5	642150.47	608880.95	573	103.615	66.5	23.48	2021
11	WD1	643513.36	609132.71	492	25.89	55	7.73	2021
12	WD2	644074.9	608429.77	494	26.51	58	7.85	2021
13	BH1	648789.46	607947.26	454.5	61.9	57.15	8.508	2022
14	BH2	648965.9	611672.02	637.5	58.05	110	0.648	2022
15	BH3	645126.58	611998.2	503	66.8	40.65	83.36	2022
16	BH4	637043.28	616381.77	527.5	26.4	12.76	2.219	2022
17	BH5	641338.54	620925.06	515.45	93.395	50.88	0.87	2022
18	WI1	639201.68	610166.45	458	106	67	25.3	2022
19	WI2	640991.53	608288.97	640.9	98.9	98.5	23.7	2022
20	WI3	641969.19	608919.29	508	101	92.5	24.5	2022
21	WI4	642081.89	608892.92	531	110	72	23.5	2022
22	WI5	642150.47	608880.95	514	111	74.5	23.15	2022
23	WD1	643513.36	609132.71	489	24.706	53.583	4.379	2022
24	WD2	644074.9	608429.77	495	28.085	62.75	4.46	2022

Two summary tables were also created - one for cations and one for anions - including the minimum, first quartile (Q1), median, third quartile (Q3), and maximum values, together with the admissible limits defined by the Romanian legislation. In this form, the figures and tables complement each other by providing both a visual and a numerical description of the hydrochemical distributions.

To further evaluate the ionic relationships, two classical hydrochemical diagrams were used: the Piper diagram, which helps identify the dominant facies, and the Schoeller - Berkaloff diagram, applied to a smaller set of representative wells. These diagrams illustrate how the major ions appear together and whether the chemical structure of the groundwater remains stable between the two sampling years.

To describe the ionic composition of the groundwater, the Piper diagram was used, which required a basic processing of the major ion data before plotting [30]. The concentrations of the major ions were first expressed in mg·L^{-1} and then converted to milliequivalents per liter (meq·L^{-1}) using the general relation [30, 31]:

$$meq/L = \frac{mg/L}{equivalent\ weight} \quad (1)$$

The equivalent weights used were: Ca^{2+} (20.04), Mg^{2+} (12.15), Na^{+} (23), K^{+} (39.1), HCO_3^- (61), Cl^- (35.45), SO_4^{2-} 48.03) and NO_3^- (62) [31]. After conversion, the ionic values were normalized to relative percentages (% meq). For cations (Ca^{2+}, Mg^{2+}, Na^{+}+ K^{+}), the percentage of each ion was calculated with respect to the total cationic charge [5, 32]:

$$X\% = \frac{X_{meq}}{Ca_{meq}+Mg_{meq}+(Na_{meq}+K_{meq})} \times 100 \quad (2)$$

For anions, the same procedure was used, based on the groupings required in the Piper plot (HCO_3^- + NO_3^-, Cl^-, SO_4^{2-}) [32]:

$$Y\% = \frac{Y_{meq}}{(HCO3_{meq}+NO3_{meq})+Cl_{meq}+SO4_{meq})} \times 100 \quad (3)$$

The Schoeller-Berkaloff diagram was prepared using the same meq·L^{-1} values, without additional steps. The ions were plotted on a logarithmic scale, one axis for each ion, following the classical approach proposed by Schoeller [20, 33], which helps to compare the ions between samples and to notice deviations from the general pattern.

RESULTS AND DISCUSSION

The section presents both the statistical distribution of the major ions and the hydrochemical facies analysis, allowing the comparison of the 2021-2022 datasets and the identification of the dominant ionic structure.

Statistical analysis of major ions

The statistical analysis is based on the annual average values from 2021 and 2022, which show, in general, a similar behavior of the major ions in the aquifer. The cations and anions stay within comparable limits in both years, and the differences appear mainly in a few wells where higher concentrations are recorded. Since the monitoring points are the same in both years, their direct comparison allows the observation of local variations without requiring additional processing

Cations

The analysis of Ca^{2+} in Figure 2a shows that the distribution in the two years remains quite similar, with medians of 117.45 mg·L^{-1} in 2021 and 108.5 mg·L^{-1} in 2022. The difference does not indicate a major change, even if in 2021 a value much higher than the rest appears (232 mg·L^{-1}), this being the outlier in the boxplot, indicating a local behavior. This suggests that Ca^{2+} follows the same general pattern in both years, and the isolated high value is linked to local conditions rather than a change in the aquifer.
Also from Figure 2b, it can be observed that magnesium (Mg^{2+}) does not vary too much between the two years. The values are relatively grouped, with close medians (39.33 mg·L^{-1} in 2021 and 42.63 mg·L^{-1} in 2022). The concentrations from the boxplot outliers in 2021 and 2022 are local variations that remain in both years. This exceedance

is present at the same well (BH3), which indicates a local behavior. At the scale of the whole analysis, the dispersion is small, with no notable changes.

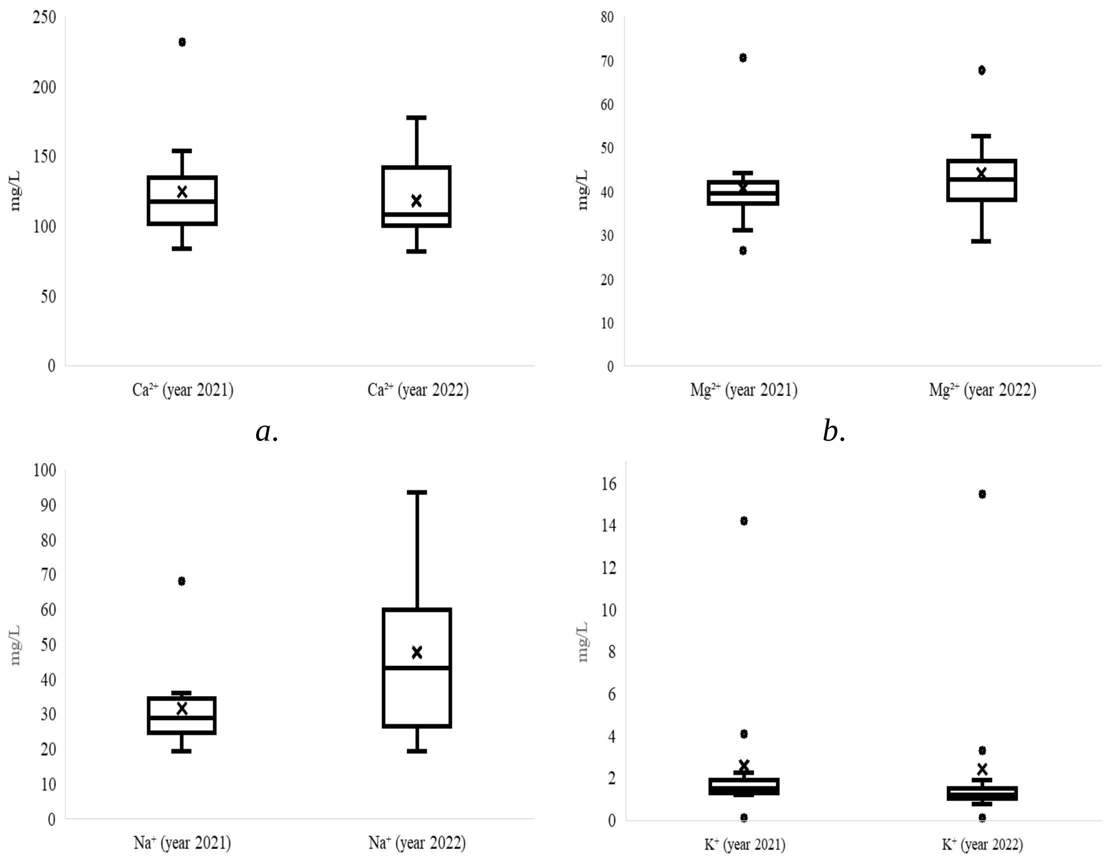

a. *b.*

c. *d.*

Figure 2. *Statistical distribution of the main cations in groundwater, represented through boxplots for: (a) calcium (Ca^{2+}), (b) magnesium (Mg^{2+}), (c) sodium (Na^{+}), and (d) potassium (K^{+}), based on the datasets from 2021 and 2022*

According to Figure 2c and Table 3, it can be observed that in the analysis of the Na^{+} ion, in 2022 the concentrations tend to be higher, and the median reaches 43.15 $mg{\cdot}L^{-1}$, compared to 29 $mg{\cdot}L^{-1}$ in 2021. A wider interval is also visible, with a maximum of 93.5 $mg{\cdot}L^{-1}$. The values are still well below the normative limit of 200 $mg{\cdot}L^{-1}$, but the difference between the two years suggests a local influence, not a generalized one. This increase is limited to a few wells and does not indicate a general shift in the aquifer.
Figure 2d shows that the K^{+} ion generally has very low values in almost all points. It can be observed, however, that in each year there is one higher value (14 - 15 $mg{\cdot}L^{-1}$), present at the same analyzed well (BH2), which separates itself from the main group. The rest of the values are generally compact, and the medians are similar, meaning that the main process does not vary. The repeated higher value at the same point suggests a local influence, while the general distribution remains stable.

Table 3. *Major cations measured in the groundwater samples (2021-2022)* [29]

Ion	Admissible limit	Year	Min	Q1	Median	Q3	Max
Ca^{2+} [$mg \cdot L^{-1}$]	No specific limit	2021	84	101.61	117.45	134.74	232
		2022	82.1	100.48	108.5	142.26	178
Mg^{2+} [$mg \cdot L^{-1}$]	No limit (included in total hardness concept)	2021	26.25	37.08	39.33	41.88	70.45
		2022	28.45	38	42.63	46.75	67.55
Na^{+} [$mg \cdot L^{-1}$]	200 $mg \cdot L^{-1}$	2021	19.5	24.75	29	34.55	68.1
		2022	19.5	26.43	43.15	59.95	93.5
K^{+} [$mg \cdot L^{-1}$]	No limit	2021	0.1	1.28	1.5	1.92	14.2
		2022	0.1	1.01	1.23	1.53	15.5

Anions

The main anions are analyzed, in order to observe the stability of their distributions and the possible differences between the two years.

According to the analysis of Figure 3a, HCO_3^- remains the dominant anion without exception.

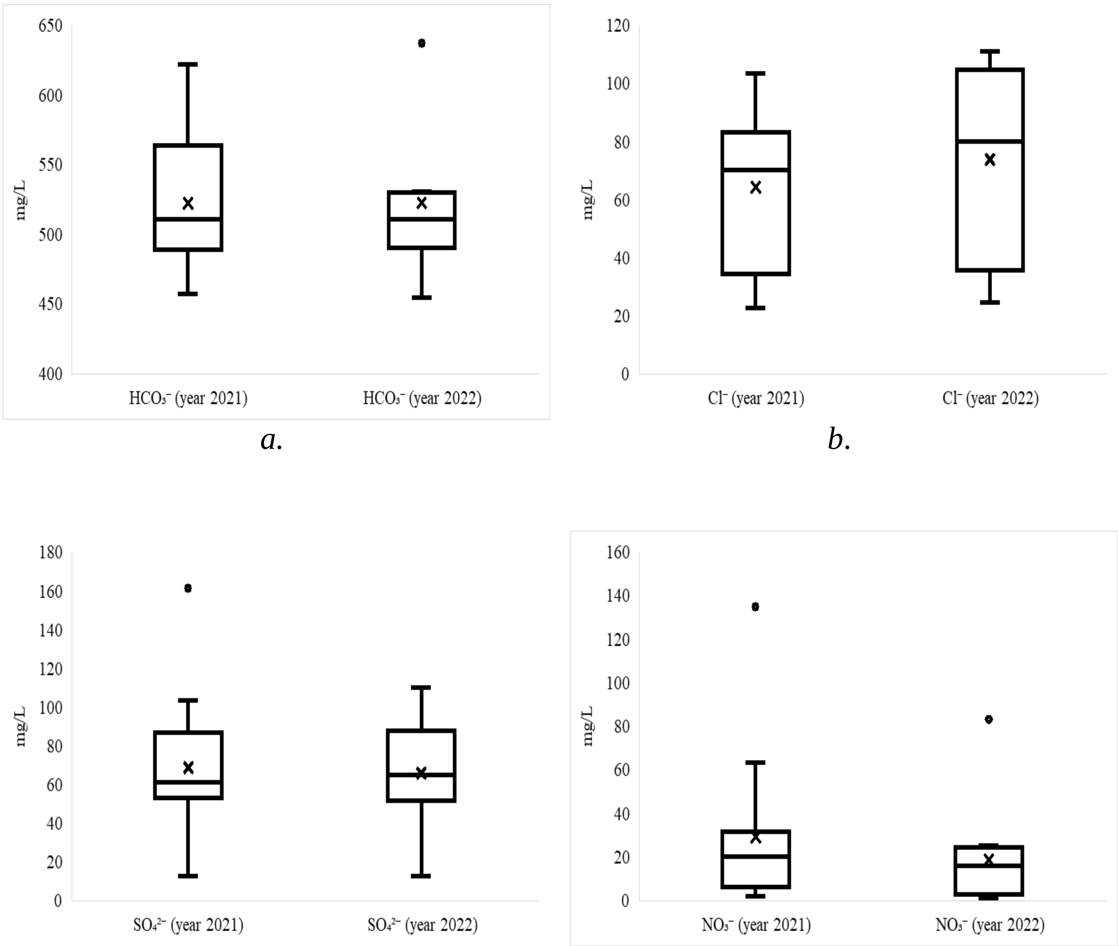

a. *b.*

c. *d.*

Figure 3. *Statistical distribution of the main anions in groundwater, represented through boxplots for: (a) bicarbonate (HCO_3^-), (b) chloride (Cl^-), (c) sulfate (SO_4^{2-}), and (d) nitrate (NO_3^-), based on the datasets from 2021 and 2022*

According to Table 4, the medians of the two years are very close (approx. 511 mg·L^{-1}), and the distribution, even if it differs slightly at the ends, does not show a change in the chemical regime. The differences appear rather in the upper part of the interval, where 2022 shows a few slightly higher values. This behavior is typical for a stable shallow aquifer and does not indicate any chemical shift.

Table 4. *Major anions measured in the groundwater samples (2021-2022)* [29]

Ion	Admissible limit	Year	Min	Q1	Median	Q3	Max
HCO_3^- [mg·L^{-1}]	No limit	2021	457	491	510.75	554	622
		2022	454.5	493.5	511	528.38	640.9
Cl^- [mg·L^{-1}]	250 mg·L^{-1}	2021	22.65	50.19	70.1	83.24	103.62
		2022	24.71	50.56	80.1	102.25	111
SO_4^{2-} [mg·L^{-1}]	250 mg·L^{-1}	2021	12.78	54.18	61.09	73.25	161.5
		2022	12.76	52.91	64.88	79	110
NO_3^- [mg·L^{-1}]	50 mg·L^{-1}	2021	2.02	7.22	19.98	31.39	135
		2022	0.648	3.84	15.83	23.9	83.36

Regarding the analysis of the Cl^- ion in Figure 3b, the distribution remains below 250 mg·L^{-1} in both datasets. In 2022, according to Table 4, a slightly higher median (80.1 mg·L^{-1}) appears, and the dispersion seems more accentuated. This shows that some points have slightly higher concentrations, but without exceeding the admissible limit. The maximum values reach 111 mg·L^{-1}. These higher values appear only in a few locations and do not suggest a general increase in chloride.

Also, in Figure 3c the SO_4^{2-} ion shows higher values, 161.5 mg·L^{-1} in 2021 and 110 mg·L^{-1} in 2022, in the same sample point (BH2). Their repeated presence in the same location suggests a local particularity of the sediments or another punctual influence. The rest of the values are relatively stable and well below the limit of 250 mg·L^{-1}. This confirms that the variation is local, while the rest of the area remains stable.

From Figure 3d it is observed that the NO_3^- ion shows the strongest deviation. In 2021, values above the limit of 50 mg·L^{-1} appear in two sample points: 135 mg·L^{-1} and 63.23 mg·L^{-1} (BH3 and WI1). Compared to 2021, according to Table 4, a decrease of the median is observed, from 19.98 mg·L^{-1} in 2021 to 15.83 mg·L^{-1} in 2022, indicating a general decrease of the values, which is also seen in the fact that in 2022 an exceedances of the 50 mg·L^{-1} limit appears only at a single sample point (BH3). The isolated values remain an indicator that the nitrate input is local and not defining for the entire area.

Looking at all the statistical results together, the ions keep the same order in both years, and most values stay close from one year to the next. The higher concentrations that appear at a few wells are isolated and repeat in the same locations, which indicate local influences rather than a change in the aquifer. The higher K^+ values appear in the same well located near an anthropized area, and the NO_3^- exceedances also occur near local settlements, which supports the idea of local inputs. Taken together, these observations show that the aquifer keeps a stable chemical behavior, with only small local variations

Hydrochemical facies analysis

To check if these local variations affect the general chemical pattern, the ion distributions were also examined in Piper and Schoeller-Berkaloff diagrams. Because the main ions keep similar levels in both years, the chemical facies is expected to remain the same, and the diagrams confirm this.

The average ion values for the two years are shown in Table 5, where Ca^{2+} has the highest levels among the cations, followed by Mg^{2+}, while Na^{+} + K^{+} stays lower. HCO_3^- is dominant in both years, and Cl^- and SO_4^{2-} appear at smaller amounts. The differences between 2021 and 2022 are small. These proportions show that the ionic structure remains almost the same in both years.

Table 5. *Mean ionic percentages (% meq) for the two sampling years*

Ion group	2021	2022
Ca^{2+}	55.7	50.7
Mg^{2+}	31.2	31.6
Na^{+}+K^{+}	13.1	17.7
HCO_3^- + NO_3^-	74.3	72.7
Cl^-	14.3	16.4
SO_4^{2-}	11.4	10.9

For the facies analysis, the annual mean values expressed in $meq \cdot L^{-1}$, shown in Table 6, were used to plot the Piper and Schoeller diagrams.

Table 6. *Mean ion concentrations expressed in $meq \cdot L^{-1}$(2021-2022)*

Year	Ca^{2+} [$meq \cdot L^{-1}$]	Mg^{2+} [$meq \cdot L^{-1}$]	Na^{+} [$meq \cdot L^{-1}$]	K^{+} [$meq \cdot L^{-1}$]	HCO_3^- [$meq \cdot L^{-1}$]	NO_3^- [$meq \cdot L^{-1}$]	Cl^- [$meq \cdot L^{-1}$]	SO_4^{2-} [$meq \cdot L^{-1}$]
2021	6.22	3.34	1.38	0.07	8.57	0.47	1.81	1.43
2022	5.89	3.62	2.08	0.06	8.57	0.3	2.08	1.37

The Piper diagram presented in Figure 4 shows that the samples from 2021 and 2022 fall in almost the same place.

Most points group in the Ca–HCO_3^- field. Ca^{2+} and Mg^{2+} dominate the cations, while HCO_3^- is the main anion. In 2022, Na^{+} + K^{+} and Cl^- are slightly higher at a few wells, but the general position of the samples stays the same. The overlap of the points shows that the groundwater chemistry is stable. The diagram confirms the same Ca–HCO_3^- facies in both years, and the small differences seen at a few points do not change the overall chemical structure.

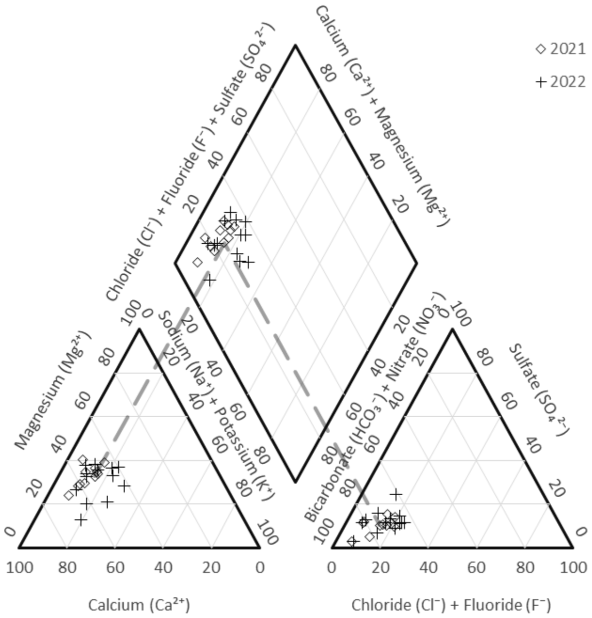

Figure 4. *Piper diagram for the major ions in 2021 and 2022*

The Schoeller diagram from Figure 5 shows the same pattern for 2021 and 2022 and keep almost the same shape. Small differences at Na^+, Cl^- and NO_3^- appear at a few points, but they do not change the overall trend. HCO_3^- remains the main anion, and Ca^{2+} and Mg^{2+} remain the main cations. The similar line shape confirms that the chemistry remains stable and follows the same pattern in both years.

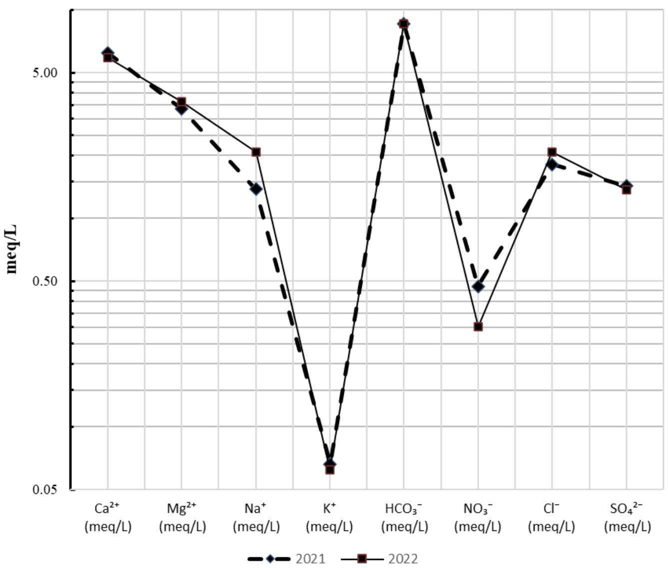

Figure 5. *Schoeller–Berkaloff diagram for the major ions (2021-2022)*

Taken together, the two diagrams show a stable Ca–HCO_3^- facies. The small deviations seen at a few wells remain local and do not affect the general picture. The chemical structure stays the same in the two years, which matches the behavior seen in the statistical results

CONCLUSIONS

The data from the two years point in the same direction. The ions keep roughly the same order, and the few higher values appear only in some wells, where the local setting seems to influence the chemistry. Small changes in Na^+, K^+, Cl^- or NO_3^- do not affect the overall behaviour of the aquifer. Both diagrams used in the study place the water in the same Ca–HCO_3^- field. In general, the aquifer behaves in a stable way, and the variations seen in a few places stay local. These observations can be used further for future checks in this alluvial sector.

REFERENCES

1. Domenico, P.A., Schwartz, F.W.: *Physical and chemical hydrogeology*, John Wiley & Sons, **1997**;
2. Al-Shaibani, A.M.: Hydrogeology and hydrochemistry of a shallow alluvial aquifer, western Saudi Arabia, *Hydrogeology Journal*, **2008**, **16**, 155-165;
3. Devic, G., Djordjevic, D., Sakan, S.: Natural and anthropogenic factors affecting the groundwater quality in Serbia, *Science of the Total Environment*, **2014**, 933-942;
4. Fetter, C.W., Boving, T., Kreamer, D.: *Contaminant hydrogeology*, Waveland Press, **2017**;
5. Fetter, C.W., Kreamer, D.: *Applied hydrogeology*, Waveland Press, **2021**;
6. Jun, X., Jin, Z.D., Wang, J.: Assessment of the Hydrogeochemistry and Groundwater Quality of the Tarim River Basin in an Extreme Arid Region, NW China, *Environmental Management*, **2013**, **53**;
7. Li, F., Pan, G., Tang, C., Zhang, Q., Yu, J.: Recharge Source and Hydrogeochemical Evolution of Shallow Groundwater in a Complex Alluvial Fan System, Southwest of North China Plain, *Environmental Geology*, **2008**, **55**, 1109-1122;
8. Singh, N., Singh, R., Kamal, V., Sen, R.: Assessment of hydrogeochemistry and the quality of groundwater in 24-Parganas districts, West Bengal, *Environmental Earth Sciences*, **2014**;
9. Selmane, T., Dougha, M., Djerbouai, S. Djamaleddine, D., Nadjet, L. Groundwater quality evaluation based on water quality indices (WQI) using GIS: Maadher plain of Hodna, Northern Algeria, *Environmental Science and Pollution Research*, **2023**, **30**, 30087-30106;
10. Tefera, A., Wassie, A., Sinshaw, B., Defersha, D., Takele, T., Atanaw, S., Tesfaye, A., Getu, E., Fenta, H., Atinkut, H., Enku, T., Sahlu, D., Melesse, A.: Groundwater quality evaluation of the alluvial aquifers using GIS and water quality indices in the Upper Blue Nile Basin, Ethiopia, *Groundwater for Sustainable Development*, **2021**, **14**, 100636;
11. Wambui, G.T., Wandubi, D.E., Njuguna, K.Z., Ochieng, O.D., Muchori, G.C.: Hydrogeochemical Characterization and Water Quality Index-Based Evaluation of Groundwater for Drinking, Livestock, and Irrigation Use in the Arid Ewaso Ng'iro-Lagh Dera Basin, Kenya, *Hydrology*, **2025**, **12**, 160;
12. Madasamy, S., Rajendiran, T., Ganesh, N., Sabarathinam, C., Panda, B., Vetrimurugan, E., Ghai, M., Singh, D.: Geochemical characterization of groundwater and water quality assessment for sustainable management of hard rock aquifer in South India, **2021**;
13. Fitts, C.R.: *Groundwater Science*, Academic Press, **2022**;
14. Gamar, A., Khiya, Z.: Hydrogeochemical Characterization Using Piper Diagram of the Groundwater Surrounding the Wild Dump of the El Hajeb Town, Morocco, *Journal of Advances in Environmental Health Research*, **2025**, **13**, 104-113;
15. Madene, E., Boufekane, A., Meddi, M.: Les nitrates dans les eaux souterraines de la nappe du Moyen Cheliff oriental et possibilités de traitement, in *Abstracts of 1st International Conference on Chemical Maters and Environment Preservation* (IC-CMEP'22 February 22 – 23, 2022, Ouargla, Algeria), **2022**;

16. Mebarki, S., Kendouci, M.A., Bendida, A.: Monitoring the spatial evolution of groundwater quality during its diversion in the drinking water supply network in arid areas, case of Bechar city (Algeria Sahara), *Applied Water Science*, **2024**, **14**;
17. Islam, A., Shen, S., Haque, M., Bodrud-Doza, M., Maw, K., Habib, M.: Assessing groundwater quality and its sustainability in Joypurhat district of Bangladesh using GIS and multivariate statistical approaches, *Environment Development and Sustainability*, **2018**, **20**, 1935-1959;
18. Jakeman, A.J., Barreteau, O., Hunt, R.J., Rinaudo, J.-D., Ross, A., Arshad, M., Hamilton, S.: Integrated groundwater management: an overview of concepts and challenges, in: *Integrated Groundwater Management*, **2016**, 3-20;
19. Júnez-Ferreira, H.E., Hernández-Hernández, M.A., Herrera, G.S., González-Trinidad, J., Cappello, C., Maggio, S., De Iaco, S.: Assessment of changes in regional groundwater levels through spatio-temporal kriging: application to the southern Basin of Mexico aquifer system, *Hydrogeology Journal*, **2023**, **31** (6), 1405-1423;
20. Schoeller, H.: Qualitative evaluation of groundwater resources, *Methods and Techniques of Groundwater Investigations and Development*, UNESCO, **1965**, 5483;
21. Scradeanu, M., Iordache, V., Palcu, M., Scradeanu, D.: Analysis of correlation between the state of groundwater and the state of terrestrial ecosystems including wetlands, *Proceedings Book of INCD ECOIND – International Symposium – SIMI 2016 "The Environment and the Industry"*, **2016**;
22. Todd, D.: *Ground Water Hydrology*, Wiley, New York, **1980**;
23. Comitetul de Stat al Geologiei, I.G.: *Harta Geologică a României*, Foaia L-25-IX,13 Piatra Neamț, București, **1968**;
24. Posea, G.: *Geomorfologia României*, București, **2002**;
25. Bogdan, P.-L., Nedeff, V., Barsan, N., Panainte-Lehaduș, M., Chitimus, D., Nedeff, F., Tomozei, C.: Applications of the GIS and Remote Sensing methods in the Land use and cover maps. Case study: Roman city and the surroundings of the Northern side area, *8th International Conference on Energy Efficiency and Agricultural Engineering (EE&AE)*, **2022**, 1-5;
26. Comitetul de Stat al Apelor, IFFA, SG: *Studiu hidrogeologic definitiv al postului de ordinul I Roman*, Arhiva ABA Siret Bacău, **1968**;
27. Administrația Națională Apele Române - Administrația Bazinală de Apă Siret: *Date hidrologice și hidrogeologice*, Arhiva ABA Siret Bacău, **2022**;
28. *** *Directive 2006/118/EC on the protection of groundwater against pollution and deterioration*, Official Journal of the European Union, **2006**, 372, 19-31;
29. Government of Romania: *Ordinance No. 7 of January 18, 2023, regarding the quality of water intended for human consumption*, Monitorul Oficial No. 63, **2023**;
30. Piper, A.M.: A graphic procedure in the geochemical interpretation of water-analyses, *EOS Transactions American Geophysical Union*, **1944**, **25** (6), 914-928;
31. Freeze, R.A., Cherry, J.A.: *Groundwater*, Prentice-Hall, Englewood Cliffs, N.J., **1979**, 161-177;
32. Hem, J.D.: *Study and Interpretation of the Chemical Characteristics of Natural Water*, USGS Water Supply Paper, 2254, **1985**;
33. Schoeller, H.: *Les eaux souterraines, Hydrologie dynamique et chimique, Recherche, Exploitation et Evaluation des Ressources*, Masson & Cie, Paris, **1962**.